King's Research Portal

[Link to publication record in King's Research Portal](#)

npg

ORIGINAL ARTICLE

Lemur tyrosine kinase-2 signalling regulates kinesin-1 light chain-2 phosphorylation and binding of Smad2 cargo

C Manser[1,4], F Guillot[1,4], A Vagnoni[1], J Davies[1], K-F Lau[1,2], DM McLoughlin[1,3], KJ De Vos[1] and CCJ Miller[1]

[1]Department of Neuroscience P037, MRC Centre for Neurodegeneration Research, Institute of Psychiatry, King's College London, Denmark Hill, London, UK; [2]Department of Biochemistry, The Chinese University of Hong Kong, Shatin, New Territories, Hong Kong and [3]Department of Psychiatry, Trinity College Institute of Neuroscience, St Patrick's Hospital, Dublin, Ireland

A recent genome-wide association study identified the gene encoding lemur tyrosine kinase-2 (*LMTK2*) as a susceptibility gene for prostate cancer. The identified genetic alteration is within intron 9, but the mechanisms by which LMTK2 may impact upon prostate cancer are not clear because the functions of LMTK2 are poorly understood. Here, we show that LMTK2 regulates a known pathway that controls phosphorylation of kinesin-1 light chain-2 (KLC2) by glycogen synthase kinase-3β (GSK3β). KLC2 phosphorylation by GSK3β induces the release of cargo from KLC2. LMTK2 signals via protein phosphatase-1C (PP1C) to increase inhibitory phosphorylation of GSK3β on serine-9 that reduces KLC2 phosphorylation and promotes binding of the known KLC2 cargo Smad2. Smad2 signals to the nucleus in response to transforming growth factor-β (TGFβ) receptor stimulation and transport of Smad2 by kinesin-1 is required for this signalling. We show that small interfering RNA loss of LMTK2 not only reduces binding of Smad2 to KLC2, but also inhibits TGFβ-induced Smad2 signalling. Thus, LMTK2 may regulate the activity of kinesin-1 motor function and Smad2 signalling.
Oncogene (2012) 31, 2773–2782; doi:10.1038/onc.2011.437; published online 26 September 2011

Introduction

Lemur tyrosine kinase-2 (LMTK2) also known as brain-enriched kinase, apoptosis-associated tyrosine kinase-2, kinase/phosphatase/inhibitor-2, cyclin-dependent kinase-5 (cdk5)/p35-regulated kinase and KIAA1079 is member of the lemur family of kinases (Wang and Brautigan, 2002; Kesavapany *et al.*, 2003; Kawa *et al.*, 2004). These are a structurally unique group of membrane-associated kinases comprising LMTK1, LMTK2 and LMTK3. All are anchored in the membrane by two predicted membrane spanning regions located at their extreme amino-termini (a splice isoform of LMTK1 lacks these sequences, but associates with membranes by palmitoylation) and contain an amino-terminally located kinase domain with a long carboxy-terminal 'tail' (Tomomura *et al.*, 2007). As such, they have been named after lemurs, the long-tailed Madagascan primates. Although originally predicted to be a dual-specificity serine–threonine/tyrosine kinase, several studies have shown that LMTK2 only targets serine and threonine residues (Wang and Brautigan, 2002, 2006; Kawa *et al.*, 2004).

Recently, *LMTK2* has become the focus of interest with its identification as a susceptibility gene for prostate cancer (Eeles *et al.*, 2008; Fitzgerald *et al.*, 2009; Waters *et al.*, 2009). Somatic mutations in *LMTK2* have also been described in other cancers (Greenman *et al.*, 2007). The identified genetic alteration is within intron 9 of the *LMTK2* gene, but the mechanism by which this increases the risk for prostate cancer is unknown. This is largely because the functions of LMTK2 are not properly understood. LMTK2 knockout mice are viable, but males are infertile owing to defects in spermatogenesis involving development of the acrosome (Kawa *et al.*, 2006). However, LMTK2 is expressed in most if not all tissues and this suggests that it has other physiological roles (Wang and Brautigan, 2002; Kesavapany *et al.*, 2003; Kawa *et al.*, 2004; Tomomura *et al.*, 2007). Indeed, there is evidence that LMTK2 is involved in endocytic recycling and in neurons, in nerve growth factor signalling and neurite outgrowth, although the precise mechanisms by which it impacts on these processes are unclear (Kawa *et al.*, 2004; Chibalina *et al.*, 2007; Inoue *et al.*, 2008).

One clue to LMTK2 function comes from the findings that it interacts with both the cdk5 activator p35 and protein phosphatase-1C (PP1C) (Wang and Brautigan, 2002; Kesavapany *et al.*, 2003). cdk5/p35 and PP1C together function in a pathway that regulates intracellular transport of cargoes on kinesin-1 molecular motors in neurons (Morfini *et al.*, 2004). Kinesin-1 is a

2774

ubiquitously expressed molecular motor that drives transport of cargoes along microtubules. Functionally, most kinesin-1 comprises a heterotetramer of two kinesin-1 motor proteins (also known as kinesin heavy chains) and two associated kinesin-1 light chains (KLC): KLC1 and KLC2 are the two best characterised light-chain isoforms and are encoded by separate genes (Rahman *et al.*, 1998; DeBoer *et al.*, 2008; Hirokawa *et al.*, 2009). Although some cargoes can attach directly to kinesin-1 motors, many associate with the motor via KLC1 or KLC2 (Hirokawa *et al.*, 2009). As such, the mechanisms that mediate binding and release of cargoes from KLC1/KLC2 represent routes for controlling kinesin-1-directed intracellular transport; phosphorylation of KLC1 and KLC2 is one such route (Morfini *et al.*, 2002, 2004; Vagnoni *et al.*, 2011).

Glycogen synthase kinase-3β (GSK3β) phosphorylates KLC2 to cause release of cargo; as such, GSK3β activity inhibits kinesin-1 transport of at least some cargoes (Morfini *et al.*, 2002). In addition, a neuronal signalling pathway to control GSK3β phosphorylation of KLC2 has been described. This involves cdk5/p35-mediated inhibitory phosphorylation of PP1C on threonine-320 (PP1Cthr^{320}), which in turn induces inhibitory phosphorylation of GSK3β on serine-9 (GSK3βser^9). Cdk5/p35 thus inhibits GSK3β phosphorylation of KLC2 and so promotes cargo binding and transport by kinesin-1 motors (Morfini *et al.*, 2004). Whether cdk5/p35 directly phosphorylates PP1Cthr^{320} or whether it induces phosphorylation via some as yet unidentified kinase is unclear (Morfini *et al.*, 2004; Li *et al.*, 2007). Whatever the precise mechanism, phosphorylation of PP1Cthr^{320} in non-neuronal cells must involve an alternative kinase as cdk5/p35 activity is mainly restricted to neurons and muscle (Lew *et al.*, 1994; Tsai *et al.*, 1994; Fu *et al.*, 2001).

Here, we show that LMTK2 also signals via PP1Cthr^{320} and GSK3βser^9 phosphorylation to regulate KLC2 phosphorylation, and that LMTK2 promotes binding of the known KLC2 cargo Smad2 to KLC2. Smad2 signals to the nucleus in response to transforming growth factor-β (TGFβ) receptor stimulation and transport of Smad2 by kinesin-1 is required for this signalling. We also show that small interfering RNA (siRNA) knockdown of LMTK2 inhibits Smad2 signalling in response to TGFβ. As such, our results provide a novel function for LMTK2 in regulating intracellular transport.

Results

LMTK2 interacts with PP1C and induces inhibitory phosphorylation of PP1Cthr^{320}

We screened a human brain yeast two-hybrid library with the intracellular domain of LMTK2 as described previously (Chibalina *et al.*, 2007). From this screen, we obtained a single almost full-length PP1C clone (PP1C residues 5 to the C terminus). To confirm that LMTK2 interacts with PP1C, we performed immunoprecipitation assays from myc-tagged LMTK2 and PP1C co-

transfected HeLa cells using anti-myc to pull-down transfected LMTK2. PP1C co-immunoprecipitated with LMTK2 from LMTK2, but not PP1C-only transfected cells (Supplementary Figure 1A). In addition, LMTK2 contains a known PP1C binding motif (valine–threonine–phenylalanine; residues 1325–1327 in mouse LMTK2) and mutation of this site to alanine–threonine–alanine (LMTK2ala$^{1325/1327}$) reduced the interaction of LMTK2 with PP1C in the immunoprecipitation assays (Supplementary Figure 1A).

PP1C activity is negatively regulated by phosphorylation of threonine^{320} (Dohadwala *et al.*, 1994). We tested whether LMTK2 phosphorylates PP1Cthr^{320} by monitoring phosphorylation of this site using a phospho-specific PP1Cthr^{320} antibody in cells co-transfected with PP1C and either LMTK2, LMTK2ala$^{1325/1327}$ or control vector. Transfection of LMTK2 has been shown to induce increased cellular LMTK2 activity (Kesavapany *et al.*, 2003). Transfection of LMTK2 but not LMTK2ala$^{1325/1327}$ increased phosphorylation of PP1Cthr^{320} (Supplementary Figure 1B). The PP1C-binding motif in LMTK2 (residues 1325–1327) is localised some distance from the LMTK2 kinase domain (residues 136–406) and we confirmed that this mutation did not influence LMTK2 activity by performing *in vitro* kinase assays with phosphorylase b as a substrate; phosphorylase b is a known *in vitro* LMTK2 substrate (Wang and Brautigan, 2006). Both LMTK2 and LMTK2ala$^{1325/1327}$ displayed equivalent activities in these assays (Supplementary Figure 1C). To complement the above studies, we also monitored how siRNA-induced loss of LMTK2 influenced phosphorylation of PP1Cthr^{320}. Four different LMTK2 siRNAs all markedly reduced LMTK2 levels and this led to a corresponding decrease in PP1Cthr^{320} phosphorylation (Figure 1a). This effect on PP1C was not seen in cells treated with two different control siRNAs or with two different LMTK2 mismatch siRNAs, none of which influenced LMTK2 expression (Figure 1a).

Thus, LMTK2 interacts with PP1C via sequences including its consensus PP1C binding motif, and induces inhibitory phosphorylation of PP1Cthr^{320}. These findings are consistent with previous observations that identified LMTK2 as a PP1C binding partner via alternative methods and which likewise demonstrated that LMTK2 phosphorylates PP1Cthr^{320} (Wang and Brautigan, 2002).

LMTK2 inhibits phosphorylation of GSK3βser^9

PP1C controls GSK3β activity by modulating phosphorylation of GSK3βser^9 (Morfini *et al.*, 2004; Hernandez *et al.*, 2010). Phosphorylation of GSK3βser^9 inhibits GSK3β activity (Sutherland *et al.*, 1993; Stambolic and Woodgett, 1994; Cross *et al.*, 1995). Moreover, increasing cellular PP1Cthr^{320} phosphorylation (which reduces PP1C activity) induces a corresponding increase in GSK3βser^9 phosphorylation (Morfini *et al.*, 2004). As LMTK2 regulates PP1Cthr^{320} phosphorylation, we therefore enquired whether it might also regulate GSK3βser^9 phosphorylation. To do so, we
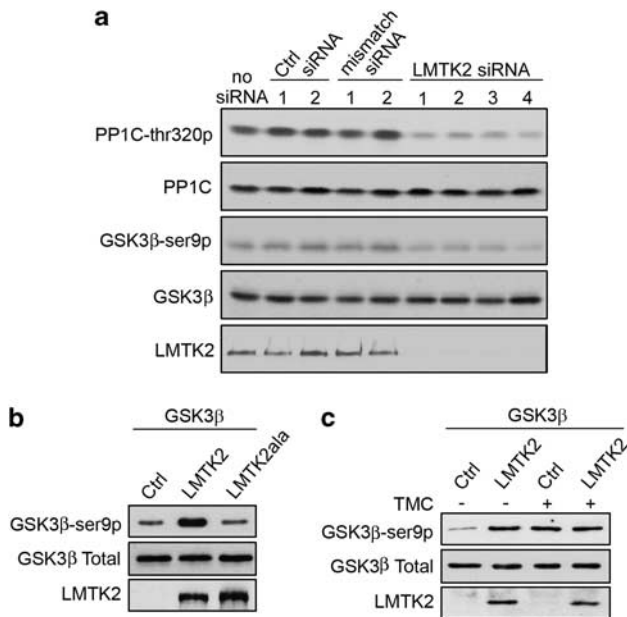
Figure 1 siRNA knockdown of LMTK2 decreases PP1Cthr^{320} and GSK3βser^9 phosphorylation and transfection of LMTK2, but not LMTK2ala$^{1325/1327}$, increases GSK3βser^9 phosphorylation in HeLa cells. (**a**) Cells were mock transfected (no siRNA), or transfected with two different control siRNAs, two different LMTK2 mismatch siRNAs or four different LMTK2 siRNAs as indicated. Samples were then probed on immunoblots for total PP1C (PP1C) and phospho-PP1Cthr^{320} (PP1C-thr320p), total GSK3β (GSK3β) and phospho-GSK3βser^9 (GSK3β-ser9p), and LMTK2 as indicated. (**b**) Cellular phosphorylation of GSK3βser^9 by LMTK2. Cells were co-transfected with GSK3β and either control vector (Ctrl), LMTK2 or LMTK2ala$^{1325/1327}$ (LMTK2ala). Samples were probed on immunoblots for total GSK3β (GSK3β), phosphorylated GSK3βser^9 (GSK3β-ser^{9}p) and LMTK2 using the myc tag. LMTK2 but not LMTK2ala$^{1325/1327}$ increased phosphorylation of GSK3βser^9. (**c**) Tautomycetin increases phosphorylation of GSK3βser^9 and does not affect LMTK2-induced phosphorylation of GSK3βser^9. Cells were co-transfected with GSK3β and either control vector (Ctrl) or LMTK2, treated with ($+$) or without ($-$) tautomycetin (TMC) as indicated and analysed on immunoblots for total GSK3β (GSK3β), phosphorylated GSK3βser^9 (GSK3β-ser^{9}p) and LMTK2 using the myc tag.

modulated LMTK2 expression in HeLa cells and monitored PP1Cthr^{320} phosphorylation by immunoblotting. Transfection of LMTK2 but not LMTK2ala$^{1325/1327}$ increased GSK3βser^9 phosphorylation (Figure 1b). We also monitored the effect of inhibiting PP1C on LMTK2-induced phosphorylation. To do so, we treated cells with tautomycetin, which is a specific inhibitor of PP1 but not PP2A (Mitsuhashi *et al.*, 2001). Tautomycetin increased GSK3βser^9 phosphorylation in a manner similar to LMTK2 and transfection of LMTK2 did not increase further this phosphorylation (Figure 1c). Finally, we monitored the effect of reducing LMTK2 expression on GSK3βser^9 phosphorylation. Knockdown of LMTK2 expression using four different siRNAs all decreased GSK3βser^9 phosphorylation (Figure 1a). Thus, elevation and siRNA knockdown of LMTK2 expression induce complementary changes in phosphorylation of both PP1Cthr^{320} and GSK3βser^9.

LMTK2 regulation of GSK3βser^9 involves PP1C

The above results are consistent with a model whereby LMTK2 exerts its effect on GSK3βser^9 via inhibitory phosphorylation of PP1Cthr^{320} and are analogous to previous studies, which show that cdk5/p35 regulation of GSK3βser^9 phosphorylation also involves PP1Cthr^{320} phosphorylation in neurons (Morfini *et al.*, 2004). Indeed, the lack of effect of LMTK2ala$^{1325/1327}$ (which is active but does not bind PP1C; Supplementary Figure 1) on GSK3βser^9 phosphorylation provides strong evidence for an involvement of PP1C in this process. However, to further eliminate the possibility that LMTK2 directly phosphorylates GSK3βser^9, we conducted *in vitro* phosphorylation studies with LMTK2 and recombinant GSK3β. LMTK2 was isolated by immunoprecipitation from LMTK2-transfected cells and equal proportions of the immunoprecipitated kinase then incubated with recombinant GSK3β or phosphorylase b substrates. In these experiments, LMTK2 phosphorylated phosphorylase b (a known LMTK2 substrate; Wang and Brautigan, 2006), but not GSK3β (Figures 2a and b). In addition, we monitored GSK3βser^9 phosphorylation in LMTK2 siRNA-treated cells that were also treated with the PP1 inhibitor tautomycetin. If LMTK2 regulates GSK3β activity via an effect on PP1C, then the reduced phosphorylation of GSK3βser^9 seen in LMTK2 siRNA-treated cells should be abolished in cells also treated with tautomycetin. This proved to be the case. Thus, tautomycetin increased GSK3βser^9 phosphorylation, but siRNA knockdown of LMTK2 in these cells had no effect on this increase. By contrast, in the absence of tautomycetin, LMTK2 knockdown decreased GSK3βser^9 phosphorylation (Figure 2c). As a control for this experiment, we monitored phosphorylation of c-jun N-terminal kinase (JNK) in the different samples. Phosphorylation of JNK is also regulated by PP1 (Mitsuhashi *et al.*, 2003), but there is no evidence to link this phosphorylation with LMTK2. Treatment with tautomycetin increased JNK phosphorylation as described previously (Mitsuhashi *et al.*, 2003), but siRNA knockdown of LMTK2 had no effect on this phosphorylation (Figure 2c). Thus, the effect of LMTK2 on GSK3βser^9 phosphorylation involves PP1C.

LMTK2 induces dephosphorylation of KLC2 and promotes binding of Smad2, a known KLC2 cargo

GSK3β phosphorylation of KLC2 is regulated by a pathway involving phosphorylation of PP1Cthr^{320} and GSK3βser^9 (Morfini *et al.*, 2004). We therefore enquired whether LMTK2 might signal to regulate KLC2 phosphorylation. To do so, we first modulated LMTK2 expression in cells and monitored phosphorylation of transfected FLAG-tagged KLC2. As the full complement of KLC2 sites phosphorylated by GSK3β *in vivo* are not known and as there are no phospho-specific antibodies that detect KLC2 phosphorylated on these sites, we monitored phosphorylation by use of Pro-Q Diamond staining of gels (Martin *et al.*, 2003) following isolation of KLC2 by immunoprecipitation using
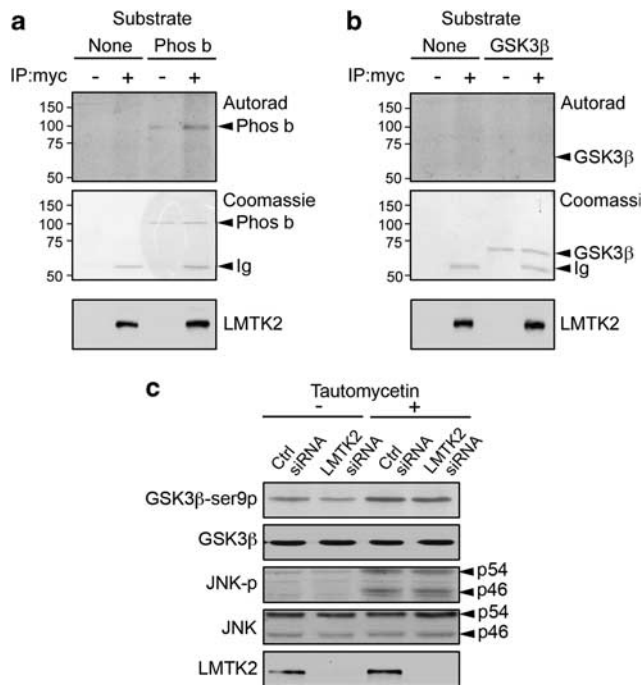
Figure 3 LMTK2 induces dephosphorylation of KLC2. (**a**) Pro-Q Diamond (Pro-Q) phospho-staining of KLC2 isolated from HeLa cells co-transfected with KLC2 and either control vector (Ctrl), LMTK2 or LMTK2ala[1325/1327] (LMTK2ala). Transfected KLC2 was isolated by immunoprecipitation using the FLAG tag and then analysed by Pro-Q Diamond phospho-staining after SDS–PAGE. Also shown are immunoblots of immunoprecipitated KLC2 (to demonstrate equal amounts of KLC2 in the different samples) and transfected LMTK2, which was detected using the myc tag. LMTK2 but not LMTK2ala[1325/1327] reduces Pro-Q Diamond staining of KLC2. (**b**) Pro-Q Diamond (Pro-Q) phospho-staining of KLC2 isolated from HeLa cells co-transfected with KLC2 and either no siRNA, control siRNA (Ctrl siRNA), LMTK2 siRNA or LMTK2 siRNA, followed by treatment with the PP1C inhibitor tautomycetin (TMC). Transfected KLC2 was isolated by immunoprecipitation using the FLAG tag, and then analysed by Pro-Q Diamond phospho-staining after SDS–PAGE. Also shown are immunoblots of immunoprecipitated KLC2 (to demonstrate equal amounts of KLC2 in the different samples) and LMTK2, which was detected using anti-LMTK2 antibody. siRNA knockdown of LMTK2 increases Pro-Q Diamond staining of KLC2 and this effect is lost following treatment of the cells with tautomycetin.

Figure 2 LMTK2 regulation of GSK3βser[9] phosphorylation involves PP1C. (**a**, **b**) *In vitro* phosphorylation ([γ-^{32}P] incorporation) of phosphorylase b, but not GSK3β by LMTK2. LMTK2 was isolated by immunoprecipitation from LMTK2-transfected cells using the myc tag. Equal proportions of immunoprecipitated LMTK2 were then incubated with phosphorylase b (**a**) or GSK3β (**b**) substrates in reactions containing [γ-^{32}P]ATP. (−) and (+) refer to the absence or presence of myc antibody in the immunoprecipitations to isolate active kinase. Reactions were also performed with no substrate as indicated. The upper panels show the autoradiographs; the lower panels are the corresponding Coomassie-stained gels to show equal amounts of substrates in the reaction mixes. Phosphorylase b and GSK3β are indicated on the Coomassie gels; Ig indicates immunoglobulin heavy chain of the immunoprecipitating antibody. Also shown (bottom panels) are immunoblots with anti-myc to demonstrate equal amounts of LMTK2 in the reaction mixes. All autorads were exposed for the same time. (**c**) Reduced GSK3βser[9] phosphorylation in LMTK2 siRNA-transfected HeLa cells in the absence, but not in the presence of the PP1C inhibitor tautomycetin. Cells were transfected with control or LMTK2 siRNAs and treated with tautomycetin as indicated. Samples were probed on immunoblots for total GSK3β (GSK3β) and phospho-GSK3βser[9] (GSK3β-ser9p) as shown. The stronger labelling for phospho-GSK3βser[9] in the presence of tautomycetin is consistent with a role for PP1C in regulating phosphorylation of this site and is in agreement with previous studies (Morfini *et al*., 2004). Also shown are control blots for total JNK (p46 and p54 isoforms) (JNK), phosphorylated JNK (JNK-p) and LMTK2 to confirm knockdown. Tautomycetin increases phosphorylation of JNK, but siRNA knockdown of LMTK2 has no effect on JNK phosphorylation.

anti-FLAG antibody. Pro-Q Diamond has now been used in numerous studies to monitor changes in protein phosphorylation (for example, Rahman-Roblick *et al*., 2008).

Co-transfection of FLAG-KLC2 with LMTK2 but not LMTK2ala[1325/1327] decreased KLC2 phosphorylation (Figure 3a). By contrast, siRNA knockdown of LMTK2 led to an increase in KLC2 phosphorylation (Figure 3b). Moreover, this increase in KLC2 phosphorylation seen in LMTK2 siRNA-treated cells was abolished in cells
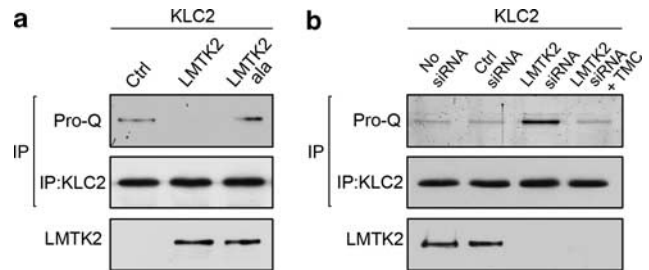
also treated with tautomycetin (Figure 3b). The lack of effect of LMTK2ala[1325/1327] on KLC2 phosphorylation and the abrogation of the LMTK2 siRNA effect on KLC2 phosphorylation with tautomycetin together provide strong support for the notion that the inhibitory effect of LMTK2 on KLC2 phosphorylation involves PP1C.

As phosphorylation of KLC2 is a mechanism for controlling its interaction with cargoes (Morfini *et al*., 2002), we investigated how LMTK2 influenced binding of KLC2 to Smad2. Smad2 is a known kinesin-1 cargo and KLC2 binding partner (Batut *et al*., 2007). Smad2 co-immunoprecipitated with FLAG-KLC2 from co-transfected cells, which is in agreement with previous studies (Batut *et al*., 2007; Figure 4a). However, co-transfection of LMTK2 to elevate expression led to an increase in the amount of Smad2 that co-immunoprecipitated with KLC2 (Figure 4a). By contrast, siRNA knockdown of LMTK2 reduced the amount of Smad2 bound to KLC2 in these immunoprecipitation assays and this effect was abrogated in cells also treated with inhibitor VIII, a specific GSK3β inhibitor (Bhat *et al*., 2003; Figure 4b). Thus, LMTK2 negatively regulates KLC2 phosphorylation and promotes its binding to Smad2, a known KLC2 cargo.

siRNA knockdown of LMTK2 inhibits TGFβ-induced Smad2 signalling
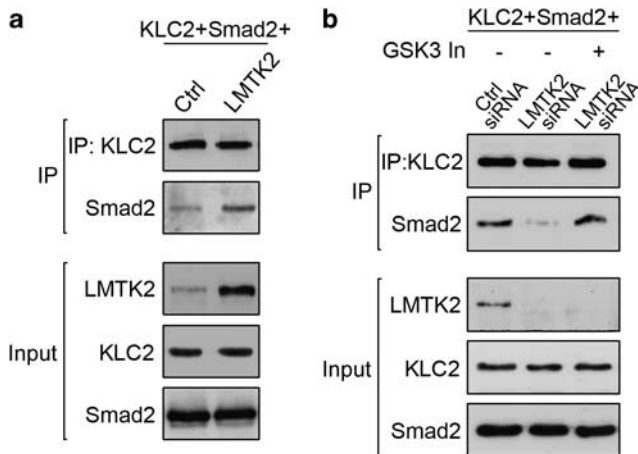Smad2 signals to the nucleus following TGFβ receptor stimulation. In response to TGFβ, Smad2 is phosphory-

Figure 4 LMTK2 increases binding of Smad2 cargo to KLC2 in HeLa cells. (**a**) Cells were co-transfected with KLC2 and Smad2, and either control vector (Ctrl) or LMTK2. KLC2 was immuno-precipitated with anti-FLAG antibody and the amounts of KLC2 and co-immunoprecipitating Smad2 then detected on immuno-blots. Upper panels (IP) show the immunoprecipitations; lower panels show the inputs in the two transfections. In the lower panel, LMTK2 was detected using rabbit anti-LMTK2 antibody. Transfection of LMTK2 increases the amount of Smad2 bound to KLC2. (**b**) Cells were co-transfected with KLC2 and Smad2, and either control siRNA (Ctrl), LMTK2 siRNA or LMTK2 siRNA, followed by treatment with GSK3β inhibitor VIII as indicated (GSK3In −/+). KLC2 was immunoprecipitated with anti-FLAG antibody and the amounts of KLC2 and co-immunoprecipitating Smad2 then detected on immunoblots. Upper panels (IP) show the immunoprecipitations; lower panels show the inputs in the two transfections. In the lower panel, LMTK2 was detected using rabbit anti-LMTK2 antibody. siRNA knockdown of LMTK2 decreases the amount of Smad2 bound to KLC2 and this effect is rescued in cells treated with GSK3β inhibitor VIII.

lated on C-terminal residues and translocates to the nucleus to regulate the transcription of Smad2-responsive genes (see for a review, Ross and Hill, 2008). Correct transport of Smad2 by kinesin-1 is required for Smad2 signalling (Batut *et al.*, 2007). As LMTK2 regulates binding of Smad2 to KLC2, we therefore enquired whether siRNA loss of LMTK2 influenced TGFβ-induced Smad2 phosphorylation, nuclear accumulation and transcriptional activity. Treatment of HeLa cells with TGFβ increased endogenous Smad2 C-terminal phosphorylation without influencing total Smad2 levels and this effect was inhibited by siRNA knockdown of LMTK2 (Figure 5a). To investigate the effect of LMTK2 on TGFβ-induced Smad2 nuclear accumulation, the subcellular distribution of Smad2 was monitored by immunostaining. TGFβ treatment in-duced nuclear accumulation of endogenous Smad2 in cells transfected with control siRNA, but this accumula-tion was inhibited in LMTK2 siRNA knockdown cells (Figure 5b). We also investigated how LMTK2 influ-enced Smad2-mediated transcription. To do so, we quantified transcriptional activity of a Smad2-respon-sive luciferase reporter gene (2xARE-Luc) in response to TGFβ stimulation in HeLa cells. TGFβ increased 2xARE-Luc activity in cells treated with control siRNA, but this increase was significantly reduced in LMTK2 siRNA knockdown cells (Figure 5c).

Two gene targets for TGFβ/Smad signalling are the cdk inhibitors *p15Ink4B* and *p21WAF1/Cip1* (Reynisdottir *et al.*, 1995). The anti-oncogenic effect of TGFβ can thus be mediated, at least in part, by increased expression of p15Ink4B and p21WAF1/Cip1, which both inhibit cell proliferation (Lee and Yang, 2001). We therefore enquired whether siRNA loss of LMTK2 influenced expression of p15Ink4B and p21WAF1/Cip1. In agreement with previous studies (Reynisdottir *et al.*, 1995), TGFβ increased the expres-sion of both p15Ink4B and p21WAF1/Cip1, but LMTK2 knockdown reduced this effect (Figure 5a). Thus, siRNA knockdown of LMTK2 inhibits TGFβ-induced Smad2 phosphorylation and nuclear signalling, including the expression of the cdk inhibitory proteins p15Ink4B and p21WAF1/Cip1.

Discussion

Here, we show that LMTK2 regulates a pathway that controls KLC2 phosphorylation and binding of Smad2 cargo. The pathway involves LMTK2 phosphorylation of PP1Cthr^{320} to inhibit PP1C activity. Loss of PP1C activity then induces inhibitory phosphorylation of GSK3βser^9 and a reduction in KLC2 phosphorylation. This lowering of KLC2 phosphorylation promotes binding of Smad2 (Figure 6). A similar pathway involving cdk5/p35 regulation of PP1C, GSK3β and KLC2 phosphorylation has been described in neurons (Morfini *et al.*, 2004). As LMTK2 also binds to p35 (Kesavapany *et al.*, 2003), it is possible that LMTK2 may, at least in part, mediate this neuronal cdk5/p35 effect on KLC2 phosphorylation (Morfini *et al.*, 2004). KLC2 is widely expressed and kinesin-1 motors function in most if not all cell types, but cdk5 is not active in many non-neuronal cells owing to the absence of p35 (Lew *et al.*, 1994; Tsai *et al.*, 1994; Fu *et al.*, 2001). Signalling to control phosphorylation of KLC2 by GSK3β cannot therefore involve cdk5/p35 in many non-neuronal cells. It thus seems likely that LMTK2 controls GSK3β phosphorylation of KLC2 in these non-neuronal cell types.

One experimental approach we utilised was to monitor PP1Cthr^{320} and GSK3βser^9 phosphorylation in cells in which LMTK2 expression was reduced using siRNAs. Despite highly efficient knockdown of LMTK2, phosphorylation of both PP1Cthr^{320} and GSK3βser^9 was lowered but not eliminated. These observations suggest that there are other pathways that control PP1Cthr^{320} phosphorylation and its regulation of GSK3βser^9. Indeed, PP1Cthr^{320} is also phosphory-lated in non-neuronal cells such as that used here by cdc2 and Nek2 (Dohadwala *et al.*, 1994; Kwon *et al.*, 1997; Helps *et al.*, 2000; Guo *et al.*, 2002).

Phosphorylation of KLC2 by GSK3β negatively regulates binding of cargoes and hence their transport on kinesin-1 motors (Morfini *et al.*, 2002). We show here that LMTK2 impacts on this process to influence binding of Smad2 to KLC2. Smad2 is a known KLC2 binding partner and kinesin-1 cargo (Batut *et al.*, 2007). Kinesin-1 is a major molecular motor that mediates
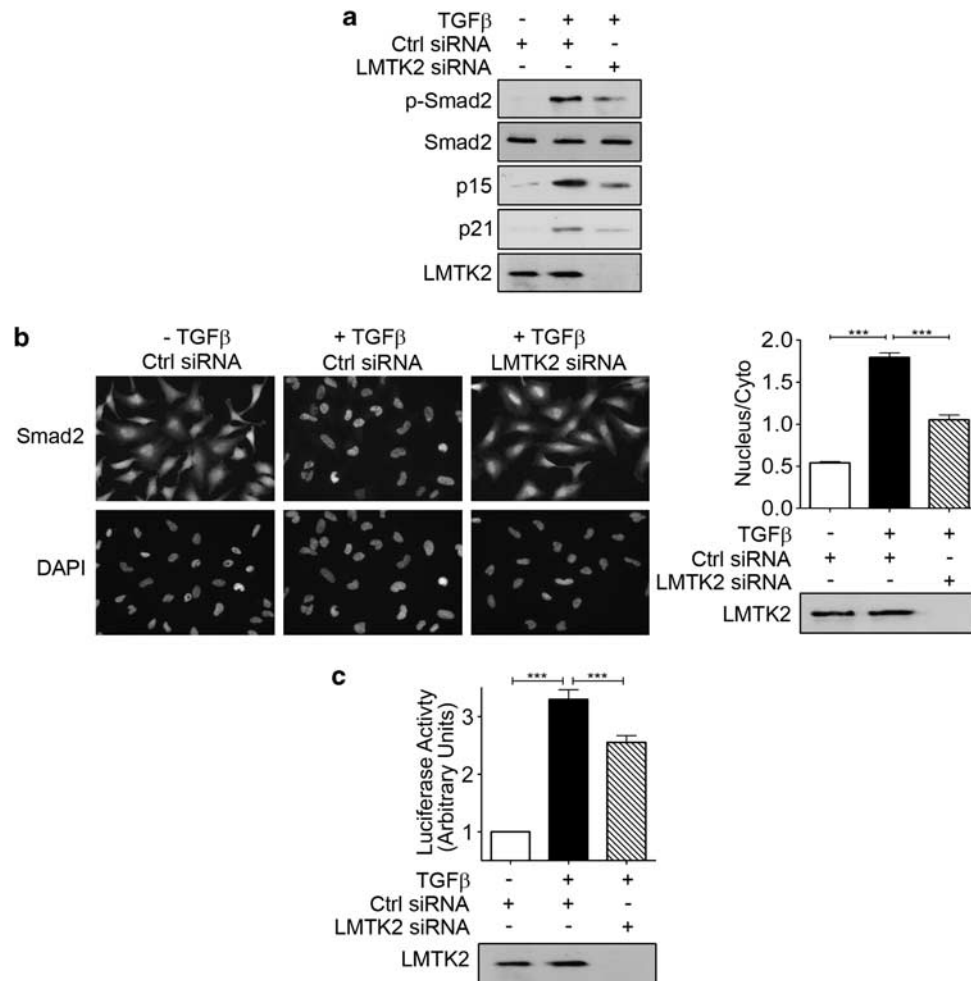
Figure 5 siRNA knockdown of LMTK2 inhibits TGFβ-induced Smad2 signalling in HeLa cells. (**a**) LMTK2 siRNA knockdown inhibits TGFβ-induced phosphorylation of Smad2 and expression of p15Ink4B and p21WAF1/Cip1. Cells were treated with either vehicle (−) or TGFβ (+) and the samples probed on immunoblots for phosphorylated (p-Smad2) and total Smad2, p15Ink4B (p15), p21WAF1/Cip1 (p21) and for LMTK2. TGFβ increases Smad2 phosphorylation and expression of p15Ink4B and p21WAF1/Cip1 in control siRNA-transfected cells (Ctrl) and these effects are inhibited in LMTK2 siRNA-transfected cells. (**b**) LMTK2 knockdown inhibits TGFβ-induced nuclear accumulation of Smad2. Cells transfected with control (Ctrl) or LMTK2 siRNAs were treated with vehicle or TGFβ as indicated and immunostained for Smad2; nuclei were labelled with 4′,6-diamidino-2-phenylindole. Bar chart shows the relative nuclear/cytoplasmic (Nucleus/Cyto) signals in the different treated cells. Statistical significance was determined by one-way analysis of variance, followed by least significant difference *post hoc* test. $N \geqslant 37$; error bars are s.e.m. ***$P < 0.0001$. Also shown is an immunoblot from cells treated at the same time as for immunostaining to demonstrate efficient siRNA knockdown of LMTK2. (**c**) LMTK2 knockdown inhibits TGFβ-induced transcription of Smad2 reporter gene *2xARE-luc*. Cells treated with control (Ctrl) or LMTK2 siRNAs were transfected with 2xARE-Luc, FoxH1 and pRL-TK (*Renilla* luciferase) plasmids and treated with vehicle or TGFβ as indicated. 2xARE-Luc signals were normalised to pRL-TK transfection efficiency control signals. TGFβ increases transcription of 2xARE-Luc and this effect is inhibited in LMTK2 siRNA knockdown cells. Statistical significance was determined by one-way analysis of variance, followed by least significant difference *post hoc* test. $N = 24$; error bars are s.e.m., ***$P < 0.0001$. Also shown is an immunoblot from cells treated at the same time as the assay to demonstrate efficient siRNA knockdown of LMTK2.

intracellular transport of numerous cargoes, including intermediate filaments, mitochondria and a variety of vesicle subtypes (Hirokawa *et al.*, 2009). As there is evidence that phosphorylation of KLC2 by GSK3β affects binding of multiple cargoes (Morfini *et al.*, 2002), it seems likely that LMTK2 may likewise influence binding of cargoes other than Smad2. LMTK2 may thus affect a number of physiological processes requiring kinesin-1-based motility.

Smad2 is required for the transduction of TGFβ signals. TGFβ induces nuclear translocation of Smad2, which in turn regulates the expression of TGFβ-responsive genes (see for reviews, Massague *et al.*, 2005; Massague and Gomis, 2006; Hill, 2009). Smad2 is transported on kinesin-1 motors through the cytoplasm and this transport is essential for Smad2 nuclear signalling (Batut *et al.*, 2007). We show that siRNA loss of LMTK2 not only reduces binding of Smad2 to KLC2, but also inhibits Smad2 nuclear signalling in response to TGFβ. Thus, loss of LMTK2 inhibits TGFβ-induced Smad2 phosphorylation, nuclear accumulation and transcription of a Smad2 reporter gene.
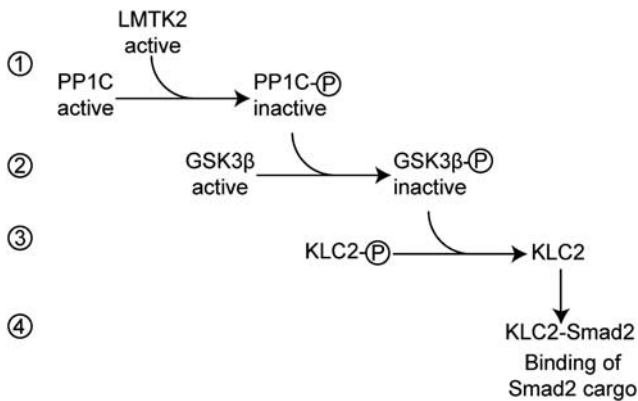
Figure 6 Model showing the proposed mechanism for LMTK2 regulation of KLC2 phosphorylation and binding of Smad2. LMTK2 directly phosphorylates PP1C on thr^{320} to reduce PP1C activity (1). Reduced PP1C activity induces an increase in inhibitory GSK3βser^9 phosphorylation (2). This lowering of GSK3β activity reduces KLC2 phosphorylation (3) to promote binding of Smad2 cargo (4).

We also show that LMTK2 loss inhibits expression of the cdk inhibitors p15Ink4B and p21WAF1/Cip1 in response to TGFβ. Some of the anti-oncogenic effects of TGFβ are believed to be mediated by the expression of these cdk inhibitory proteins (Reynisdottir et al., 1995; Lee and Yang, 2001).

Loss of LMTK2 inhibited but did not abrogate Smad2 nuclear signalling. As siRNA knockdown of LMTK2 was highly efficient, it is possible that there are other processes that may impact upon kinesin-1 transport of Smad2. Indeed, there are two KLC isoforms (KLC1 and KLC2) and only KLC2 is a target for phosphorylation by GSK3β; LMTK2 regulation of GSK3β activity will thus not influence any binding of Smad2 to KLC1. Also, the C-terminal domains of KLCs (which is where the GSK3β phosphorylation sites in KLC2 are believed to be located; Morfini et al., 2002) are altered by alternative splicing of mRNAs and this also influences binding of cargoes (Wozniak and Allan, 2006). These other regulatory mechanisms may also influence kinesin-1 transport of Smad2 and Smad2 signalling.

TGFβ signalling functions in a variety of processes, including cell division, differentiation, cell migration, inflammation and apoptosis (Massague et al., 2005; Massague and Gomis, 2006). Altered TGFβ/Smad signalling has also been associated with a number of human diseases. These include some neurodegenerative diseases such as Alzheimer's disease and amyotrophic lateral sclerosis (Town et al., 2008; Katsuno et al., 2011). Interestingly, defective axonal transport of kinesin-1 cargoes is a prominent pathological feature of these disorders (De Vos et al., 2008) and disruption to cdk5/p35 (which phosphorylates LMTK2 to regulate its activity) is also seen in Alzheimer's disease and amyotrophic lateral sclerosis (Bajaj et al., 1999; Kesavapany et al., 2003; Su and Tsai, 2011). As such, altered LMTK2 function may contribute to some neurodegenerative diseases.

In addition, TGFβ/Smad signalling has been associated with a variety of cancers (see for a review, Massague, 2008). In normal and pre-malignant cells, TGFβ suppresses tumour formation, but in later stages of tumourigenesis, TGFβ signalling may be detrimental and facilitate malignant progression (Massague, 2008).

The effects of the LMTK2 intron 9 genetic alteration associated with prostate cancer on LMTK2 function are not known. However, recent evidence indicates that LMTK2 expression may be significantly reduced in malignant prostate cancer tissues and that this may be due to the intron 9 change (Harries et al., 2010). If this proves to be the case, then LMTK2 stimulation of Smad2 binding to KLC2 and transport on kinesin-1 may be inhibited in prostate cancer cells. In addition, LMTK2 has recently been shown to associate with myosin VI and to regulate its function in cellular transport (Chibalina et al., 2007; Inoue et al., 2008). Altered expression of myosin VI has also been seen in prostate cancer (Su et al., 2001; Puri et al., 2010). Thus, LMTK2 modulates the function of two different molecular motors whose functions may impact on prostate cancer.

Materials and methods

Antibodies
The following antibodies were used: anti-Myc-tag (9B11), anti-phospho-PP1Cα (Thr320), anti-phospho-GSK3β (Ser9), anti-phospho-SAPK/JNK, anti-SAPK/JNK, anti-Smad2 (86F7), anti-phospho-Smad2 (Ser465/467) (138D4), anti-p15INK4B (all from Cell Signaling Technology, Danvers, MA, USA); anti-PP1Cα (E-9) (Santa Cruz Biotechnology, Santa Cruz, CA, USA); anti-GSK3β and anti-Smad2/3 (BD Biosciences, Franklin Lakes, NJ, USA); anti-FLAG (M5) (Sigma, Poole, UK); and anti-p21/WAF1/Cip1 (Abcam, Cambridge, UK). The rabbit LMTK2 polyclonal antibody was as described (Chibalina et al., 2007).

Plasmids
LMTK2 cDNA was generated from CD1 mouse brain by reverse transcription–polymerase chain reaction using a SuperScript III Platinum Reverse Transcription–Polymerase Chain Reaction Kit (Invitrogen, Paisley, UK) using the following primer set: 5′-GACCGCGCGGTGGACGAGA TG-3′ and 5′-GGAGTGGATTGCGTTGCTCAGGTG-3′. An myc tag was inserted onto the C terminus by polymerase chain reaction and LMTK2-myc cloned into pCIneo (Promega, Southampton, UK). To generate the LMTK2ala$^{1325/1327}$, LMTK2 valine^{1325} and phenylalanine^{1327} were both mutated to alanine using a QuikChange XL Site-Directed Mutagenesis Kit (Stratagene, Amsterdam, The Netherlands) and the following primer set: 5′-GGAAGAAGGAAAAGAAGGCA GCGACAGCTTTCGATGATGTCACCG-3′ and 5′-CGGT GACATCATCGAAAGCTGTCGCTGCCTTCTTTTCCTTC TTCC-3′. Human PP1Cα in pCMV6-XL4 was from Origene (Rockville, MD, USA). KLC2 cDNA was from Source Bioscience (Nottingham, UK); an amino-terminal FLAG tag was added by polymerase chain reaction and FLAG-KLC2 cloned into pCIneo. Plasmids for GFP-Smad2, GSK3β, forkhead activin signal transducer FAST1 (FoxH1) and 2xARE-Luc were as described previously (Lovestone et al.,

1994; Zhou et al., 1998; Noda et al., 2006; Batut et al., 2007). pRL-TK Renilla luciferase reporter control plasmid was from Promega. For controls and so that all transfections received the same amounts of DNA, pCIneo vector containing the Escherichia coli chloramphenicol acetyltransferase was used as described (Guidato et al., 1998).

Yeast two-hybrid screen

The yeast two-hybrid screen was performed using a pre-transformed human brain cDNA library (Clontech, Mountain View, CA, USA) with the cytoplasmic domain of LMTK2 (amino acids 67–1443) as the 'bait' cloned into pY1 (Chibalina et al., 2007). Methods were according to the instructions provided by Clontech. Following mating, yeast underwent tryp-/leu-/his- selection and vigorously growing clones were subjected to β-galactosidase assays. Prey plasmids were rescued by transformation into E. coli and positive plasmids identified by co-transformation back into yeast either alone or with LMTK2 bait as described elsewhere (McLoughlin and Miller, 1996).

Cell culture and transfection

HeLa cells were cultured in Dulbecco's modified Eagle's medium containing 10% fetal bovine serum and 2 mM L-glutamine (Invitrogen). Cells were transfected using Exgen 500 (Fermentas, Burlington, ON, Canada) according to the manufacturer's instructions except for immunofluorescence and reporter gene assays where Lipofectamine 2000 (Invitrogen) was used, again according to the manufacturer's instructions. Lipofectamine 2000 was used for immunostaining since Exgen can give background staining with 4′,6-diamidino-2-phenylindole, which was used as a nuclear label (see Immunofluorescence studies below). For siRNA knockdowns, cells were transfected with Oligofectamine (Invitrogen) according to the manufacturer's instructions. Human LMTK2 was targeted with four different siRNAs that were all obtained from ThermoFisher (Lafayette, CO, USA): 2068 (5′-UCAGG AGCGUUGAACUUGA-3′), 1158 (5′-GCAGGUACAAGG AGGAUUA-3′), 1262 (5′-GCAGAUCAGACUAAGUAU A-3′) and 1972 (5′-GUAGUAACUUGGAGCUUGA-3′). Unless indicated, all four siRNAs were used in combination and these gave knockdowns that were equivalent or greater than the individual siRNAs; this is in agreement with previous studies that also used these siRNAs (Chibalina et al., 2007). Control siRNAs were also from ThermoFisher. Cells were harvested for analyses 4 days after siRNA treatment. Where described, cells were treated with 5 μM tautomycetin (Merck Chemical Ltd, Beeston, UK) or 1 μM GSK3β inhibitor VIII (AR-A014418; N-(4-nethoxybenzyl)-N′-(5-nitro-1,3-thiazol-2-yl)urea) for 5 h before harvesting. TGFβ (Sigma) was used at 1 ng/ml for the times indicated.

SDS–PAGE and immunoblotting

Cells were harvested for sodium dodecyl sulfate–polyacrylamide gel electrophoresis (SDS–PAGE) by washing with phosphate-buffered saline pre-warmed at 37 °C and scraping into SDS–PAGE sample buffer and immediately heating to 100 °C. Samples were separated on 8 or 10% (w/v) acrylamide gels, transferred to Protran nitrocellulose membranes (Schleicher & Schuell, Dassel, Germany) using a Transblot system (BioRad, Hercules, CA, USA) and following blocking, probed with primary antibodies. Following washing, the blots were incubated with horseradish peroxidase-conjugated goat anti-mouse or anti-rabbit immunoglobulins and developed using an enhanced chemiluminescence system (GE Healthcare, Piscataway, NJ, USA).

Immunoprecipitation and Pro-Q Diamond staining

Immunoprecipitation assays were performed essentially as described (Vagnoni et al., 2011). Briefly, cells were lysed in ice-cold immunoprecipitation (IP) buffer comprising 20 mM HEPES (pH 7.4), 100 mM NaCl, 1% Triton X-100, 10% glycerol, 5 mM EDTA, 0.5 mM sodium orthovanadate, 25 mM sodium fluoride, 20 mM β-glycerophosphate and protease inhibitors (Complete, Roche, Burgess Hill, UK) for 30 min. Following centrifugation at 16 000 g for 30 min at 4 °C, the supernatants were pre-cleared with protein G-Sepharose beads (Sigma) for 1 h at 4 °C, and then incubated with primary antibodies for 16 h at 4 °C. Antibodies were captured with protein G-Sepharose beads and following washing with immunoprecipitation buffer, bound proteins were eluted by incubation in SDS–PAGE sample buffer and heating at 100 °C. Samples were then analysed by immunoblotting and Pro-Q Diamond staining. For Pro-Q Diamond staining, gels were incubated with Pro-Q Diamond phosphoprotein gel stain (Invitrogen) according to the manufacturer's instructions and signals captured using an Ettan DIGE Imager (GE Healthcare).

In vitro phosphorylation studies

Comparative in vitro phosphorylation studies of phosphorylase b (Sigma) by LMTK2 and LMTK2ala$^{1325/1327}$ were performed essentially as described (Kesavapany et al., 2003). Briefly, LMTK2 or LMTK2ala$^{1325/1327}$ was isolated by immunoprecipitation from either LMTK2- or LMTK2ala$^{1325/1327}$-transfected cells using antibody 9B11 to the myc tag. LMTK2/LMTK2ala$^{1325/1327}$ were then incubated with 2 μg of phosphorylase b, 0.185 MBq [γ-^{32}P]ATP in 25 mM Tris–HCl (pH 7.5) containing 10 mM MgCl$_2$, 5 mM β-glycerophosphate, 0.1 mM sodium orthovanadate, 2 mM dithiothreitol and 20 μM ATP for 20 min at 30 °C in a final volume of 30 μl. The reactions were stopped by adding SDS–PAGE sample buffer and heating to 100 °C. Samples were separated by SDS–PAGE and the gels stained with Coomassie blue (Sigma) and subjected to autoradiography. For studies testing LMTK2 phosphorylation of GSK3β, LMTK2 was again isolated by immunoprecipitation from LMTK2-transfected cells using antibody 9B11 to the myc tag. LMTK2 was then incubated with 1 μg of either phosphorylase b or GSK3β (Cell Signaling Technology), 0.185 MBq [γ-^{32}P]ATP in 25 mM Tris–HCl (pH 7.5) containing 10 mM MgCl$_2$, 5 mM β-glycerophosphate, 0.1 mM sodium orthovanadate, 2 mM dithiothreitol, 20 μM ATP and 1 μM GSK3β inhibitor VIII for 20 min at 30 °C in a final volume of 50 μl. GSK3β inhibitor VIII was included to inhibit any possible autophosphorylation of GSK3β, but was also added to phosphorylase b reactions. The reactions were again stopped by adding SDS–PAGE sample buffer and heating to 100 °C, and equal volumes of the samples separated by SDS–PAGE; the gels were then stained with Coomassie blue and subjected to autoradiography.

Luciferase reporter assays

Luciferase assays were performed essentially as described by us for other reporter gene assays (Lau et al., 2008) using a Dual-Glo luciferase assay system according to the manufacturer's instructions (Promega). Briefly, HeLa cells transfected with control or LMTK2 siRNAs were cultured for 3 days. They were then transfected with reporter gene constructs and the media replaced with Dulbecco's modified Eagle's medium containing 0.2% foetal bovine serum with or without 1 ng/ml TGFβ, and the cells were cultured for a further 16 h as described by others for similar assays (Noda et al., 2006; Murakami et al., 2009). Cells were then harvested into Glo lysis buffer (Promega) and the lysates transferred to a 96-well luminometer plate (Wallac). An equal volume of Dual-Glo

luciferase substrate was added and firefly luciferase activities produced by the firefly luciferase reporter plasmid 2xARE-Luc measured using a Wallac Trilux luminometer (Perkin Elmer, Beaconsfield, UK). *Renilla* luciferase activities produced by the co-transfected phRL-TK transfection efficiency control plasmid were then assayed by adding an equal volume of Dual-Glo Stop&Glo substrate (Promega, Southampton, UK) (comprising the stop solution for firefly luciferase and substrate for *Renilla* luciferase) and re-measuring in the luminometer. Firefly luciferase activities were normalised to the corresponding *Renilla* luciferase activities and statistical analyses performed using one-way analysis of variance with least significant difference *post hoc* test.

Immunofluorescence studies
HeLa cells were transfected with control or LMTK2 siRNAs. At 17 h before analyses, the media were replaced with Dulbecco's modified Eagle's medium containing 0.2% foetal bovine serum and the cells treated with 1 ng/ml TGFβ (Sigma) for 1 h. Cells were then fixed in 4% (w/v) paraformaldehyde in phosphate-buffered saline for 20 min, permeabilised with 0.5% (w/v) Triton X-100 in phosphate-buffered saline for 10 min, blocked with 5% (v/v) foetal bovine serum in phosphate-buffered saline for 1 h, and then probed with anti-Smad2 86F7 (Cell Signaling Technology) antibody diluted in blocking solution. Following washing, the primary antibody was detected using goat anti-rabbit immunoglobulin G coupled to Alexa Fluor 568 (Molecular Probes) and the cells were counterstained with 0.5 μg/ml 4′,6-diamidino-2-phenylindole (Sigma) to visualise nuclei. Samples were mounted in

Vectashield (Vector labs) and imaged using a Leica DM5000B microscope and ×40/0.75 HCX FLUOTAR objective (Leica Microsystems, Wetzlar, Germany). To monitor the relative amounts of Smad2 in the cytoplasm and nuclei, the mean Smad2 fluorescence signals were quantified in each compartment using Image J (developed by Wayne Rasband, NIH, Bethesda, MD, USA; http://rsb.info.nih.gov/ij/); nuclei were defined by 4′,6-diamidino-2-phenylindole staining. Analyses were performed from at least 37 cells from two different experiments. Statistical significance was determined using one-way analysis of variance with least significant difference *post hoc* test.

References

Bajaj NP, al-Sarraj ST, Leigh PN, Anderson V, Miller CC. (1999). Cyclin dependent kinase-5 (CDK-5) phosphorylates neurofilament heavy (NF-H) chain to generate epitopes for antibodies that label neurofilament accumulations in amyotrophic lateral sclerosis (ALS) and is present in affected motor neurones in ALS. *Prog Neuropsychopharmacol Biol Psychiatry* **23**: 833–850.

Batut J, Howell M, Hill CS. (2007). Kinesin-mediated transport of Smad2 is required for signaling in response to TGF-beta ligands. *Dev Cell* **12**: 261–274.

Bhat R, Xue Y, Berg S, Hellberg S, Ormo M, Nilsson Y *et al.* (2003). Structural insights and biological effects of glycogen synthase kinase 3-specific inhibitor AR-A014418. *J Biol Chem* **278**: 45937–45945.

Chibalina MV, Seaman MN, Miller CC, Kendrick-Jones J, Buss F. (2007). Myosin VI and its interacting protein LMTK2 regulate tubule formation and transport to the endocytic recycling compartment. *J Cell Sci* **120**: 4278–4288.

Cross DAE, Alessi DR, Cohen P, Andjelkovich M, Hemmings B. (1995). Inhibition of glycogen synthase kinase-3 by insulin mediated by protein kinase B. *Nature* **378**: 785–789.

DeBoer SR, You Y, Szodorai A, Kaminska A, Pigino G, Nwabuisi E *et al.* (2008). Conventional kinesin holoenzymes are composed of heavy and light chain homodimers. *Biochemistry* **47**: 4535–4543.

De Vos KJ, Grierson AJ, Ackerley S, Miller CCJ. (2008). Role of axonal transport in neurodegenerative diseases. *Annu Rev Neurosci* **31**: 151–173.

Dohadwala M, Da Cruz e Silva EF, Hall FL, Williams RT, Carbonaro-Hall DA, Nairn AC *et al.* (1994). Phosphorylation and inactivation of protein phosphatase 1 by cyclin-dependent kinases. *Proc Natl Acad Sci USA* **91**: 6408–6412.

Eeles RA, Kote-Jarai Z, Giles GG, Olama AA, Guy M, Jugurnauth SK *et al.* (2008). Multiple newly identified loci associated with prostate cancer susceptibility. *Nat Genet* **40**: 316–321.

Fitzgerald LM, Kwon EM, Koopmeiners JS, Salinas CA, Stanford JL, Ostrander EA. (2009). Analysis of recently identified prostate cancer susceptibility loci in a population-based study: associations with family history and clinical features. *Clin Cancer Res* **15**: 3231–3237.

Fu AK, Fu WY, Cheung J, Tsim KW, Ip FC, Wang JH *et al.* (2001). Cdk5 is involved in neuregulin-induced AChR expression at the neuromuscular junction. *Nat Neurosci* **4**: 374–381.

Greenman C, Stephens P, Smith R, Dalgliesh GL, Hunter C, Bignell G *et al.* (2007). Patterns of somatic mutation in human cancer genomes. *Nature* **446**: 153–158.

Guidato S, McLoughlin D, Grierson AJ, Miller CCJ. (1998). Cyclin D2 interacts with cdk-5 and modulates cellular cdk-5/p35 activity. *J Neurochem* **70**: 492–500.

Guo CY, Brautigan DL, Larner JM. (2002). Ionizing radiation activates nuclear protein phosphatase-1 by ATM-dependent dephosphorylation. *J Biol Chem* **277**: 41756–41761.

Harries LW, Perry JR, McCullagh P, Crundwell M. (2010). Alterations in LMTK2, MSMB and HNF1B gene expression are associated with the development of prostate cancer. *BMC Cancer* **10**: 315.

Helps NR, Luo X, Barker HM, Cohen PT. (2000). NIMA-related kinase 2 (Nek2), a cell-cycle-regulated protein kinase localized to centrosomes, is complexed to protein phosphatase 1. *Biochem J* **349**: 509–518.

Hernandez F, Langa E, Cuadros R, Avila J, Villanueva N. (2010). Regulation of GSK3 isoforms by phosphatases PP1 and PP2A. *Mol Cell Biochem* **344**: 211–215.

Hill CS. (2009). Nucleocytoplasmic shuttling of Smad proteins. *Cell Res* **19**: 36–46.

Hirokawa N, Noda Y, Tanaka Y, Niwa S. (2009). Kinesin superfamily motor proteins and intracellular transport. *Nat Rev Mol Cell Biol* **10**: 682–696.

Inoue T, Kon T, Ohkura R, Yamakawa H, Ohara O, Yokota J et al. (2008). BREK/LMTK2 is a myosin VI-binding protein involved in endosomal membrane trafficking. Genes Cells 13: 483–495.

Katsuno M, Adachi H, Banno H, Suzuki K, Tanaka F, Sobue G. (2011). Transforming growth factor-beta signaling in motor neuron diseases. Curr Mol Med 11: 48–56.

Kawa S, Fujimoto J, Tezuka T, Nakazawa T, Yamamoto T. (2004). Involvement of BREK, a serine/threonine kinase enriched in brain, in NGF signalling. Genes Cells 9: 219–232.

Kawa S, Ito C, Toyama Y, Maekawa M, Tezuka T, Nakamura T et al. (2006). Azoospermia in mice with targeted disruption of the Brek/Lmtk2 (brain-enriched kinase/lemur tyrosine kinase 2) gene. Proc Natl Acad Sci USA 103: 19344–19349.

Kesavapany S, Lau K-F, Ackerley S, Banner S, Shemilt SJA, Cooper JD et al. (2003). Identification of a novel, membrane-associated neuronal kinase, cdk5/p35 regulated kinase (cprk). J Neurosci 23: 4975–4983.

Kwon YG, Lee SY, Choi Y, Greengard P, Nairn AC. (1997). Cell cycle-dependent phosphorylation of mammalian protein phosphatase 1 by cdc2 kinase. Proc Natl Acad Sci USA 94: 2168–2173.

Lau KF, Chan WM, Perkinton MS, Tudor EL, Chang RC, Chan HY et al. (2008). Dexras1 interacts with FE65 to regulate FE65-amyloid precursor protein dependent transcription. J Biol Chem 283: 34728–34737.

Lee MH, Yang HY. (2001). Negative regulators of cyclin-dependent kinases and their roles in cancers. Cell Mol Life Sci 58: 1907–1922.

Lew J, Huang Q-Q, Zhong Q, Winkfein RJ, Aebersold R, Hunt T et al. (1994). A brain-specific activator of cyclin-dependent kinase 5. Nature 371: 423–426.

Li T, Chalifour LE, Paudel HK. (2007). Phosphorylation of protein phosphatase 1 (PP1) by cyclin-dependent protein kinase 5 during nerve growth factor-induced PC12 cell differentiation. J Biol Chem 282: 6619–6628.

Lovestone S, Reynolds CH, Latimer D, Davis DR, Anderton BH, Gallo J-M et al (1994). Alzheimer's disease-like phosphorylation of the microtubule-associated protein tau by glycogen synthase kinase-3 in transfected mammalian cells. Curr Biol 4: 1077–1086.

Martin K, Steinberg TH, Cooley LA, Gee KR, Beechem JM, Patton WF. (2003). Quantitative analysis of protein phosphorylation status and protein kinase activity on microarrays using a novel fluorescent phosphorylation sensor dye. Proteomics 3: 1244–1255.

Massague J. (2008). TGFbeta in cancer. Cell 134: 215–230.

Massague J, Gomis RR. (2006). The logic of TGFbeta signaling. FEBS Lett 580: 2811–2820.

Massague J, Seoane J, Wotton D. (2005). Smad transcription factors. Genes Dev 19: 2783–2810.

McLoughlin DM, Miller CCJ. (1996). The intracellular cytoplasmic domain of the Alzheimer's disease amyloid precursor protein interacts with phosphotyrosine binding domain proteins in the yeast two-hybrid system. FEBS Lett 397: 197–200.

Mitsuhashi S, Matsuura N, Ubukata M, Oikawa H, Shima H, Kikuchi K. (2001). Tautomycetin is a novel and specific inhibitor of serine/threonine protein phosphatase type 1, PP1. Biochem Biophys Res Commun 287: 328–331.

Mitsuhashi S, Shima H, Tanuma N, Matsuura N, Takekawa M, Urano T et al. (2003). Usage of tautomycetin, a novel inhibitor of protein phosphatase 1 (PP1), reveals that PP1 is a positive regulator of Raf-1 in vivo. J Biol Chem 278: 82–88.

Morfini G, Szebenyi G, Brown H, Pant HC, Pigino G, DeBoer S et al. (2004). A novel CDK5-dependent pathway for regulating GSK3 activity and kinesin-driven motility in neurons. EMBO J 23: 2235–2245.

Morfini G, Szebenyi G, Elluru R, Ratner N, Brady ST. (2002). Glycogen synthase kinase 3 phosphorylates kinesin light chains and negatively regulates kinesin-based motility. EMBO J 21: 281–293.

Murakami M, Kawachi H, Ogawa K, Nishino Y, Funaba M. (2009). Receptor expression modulates the specificity of transforming growth factor-beta signaling pathways. Genes Cells 14: 469–482.

Noda D, Itoh S, Watanabe Y, Inamitsu M, Dennler S, Itoh F et al. (2006). ELAC2, a putative prostate cancer susceptibility gene product, potentiates TGF-beta/Smad-induced growth arrest of prostate cells. Oncogene 25: 5591–5600.

Puri C, Chibalina MV, Arden SD, Kruppa AJ, Kendrick-Jones J, Buss F. (2010). Overexpression of myosin VI in prostate cancer cells enhances PSA and VEGF secretion, but has no effect on endocytosis. Oncogene 29: 188–200.

Rahman A, Friedman DS, Goldstein LS. (1998). Two kinesin light chain genes in mice. Identification and characterization of the encoded proteins. J Biol Chem 273: 15395–15403.

Rahman-Roblick R, Hellman U, Becker S, Bader FG, Auer G, Wiman KG et al. (2008). Proteomic identification of p53-dependent protein phosphorylation. Oncogene 27: 4854–4859.

Reynisdottir I, Polyak K, Iavarone A, Massague J. (1995). Kip/Cip and Ink4 Cdk inhibitors cooperate to induce cell cycle arrest in response to TGF-beta. Genes Dev 9: 1831–1845.

Ross S, Hill CS. (2008). How the Smads regulate transcription. Int J Biochem Cell Biol 40: 383–408.

Stambolic V, Woodgett JR. (1994). Mitogen inactivation of glycogen synthase kinase-3b in intact cells via serine 9 phosphorylation. Biochem J 303: 701–704.

Su AI, Welsh JB, Sapinoso LM, Kern SG, Dimitrov P, Lapp H et al. (2001). Molecular classification of human carcinomas by use of gene expression signatures. Cancer Res 61: 7388–7393.

Su SC, Tsai LH. (2011). Cyclin-dependent kinases in brain development and disease. Annu Rev Cell Dev Biol (in press).

Sutherland C, Leighton IA, Cohen P. (1993). Inactivation of glycogen synthase kinase-3b by phosphorylation: new kinase connections in insulin and growth-factor signalling. Biochem J 296: 15–19.

Tomomura M, Morita N, Yoshikawa F, Konishi A, Akiyama H, Furuichi T et al. (2007). Structural and functional analysis of the apoptosis-associated tyrosine kinase (AATYK) family. Neuroscience 148: 510–521.

Town T, Laouar Y, Pittenger C, Mori T, Szekely CA, Tan J et al. (2008). Blocking TGF-beta-Smad2/3 innate immune signaling mitigates Alzheimer-like pathology. Nat Med 14: 681–687.

Tsai L-H, Delalle I, Caviness JVS, Chae T, Harlow E. (1994). p35 is a neural-specific regulatory subunit of cyclin-dependent kinase 5. Nature 371: 419–423.

Vagnoni A, Rodriguez L, Manser C, De Vos KJ, Miller CCJ. (2011). Phosphorylation of kinesin light chain-1 at serine-460 modulates binding and trafficking of calsyntenin-1. J Cell Sci 124: 1032–1042.

Wang H, Brautigan DL. (2002). A novel transmembrane ser/thr kinase complexes with protein phosphatase-1 and inhibitor-2. J Biol Chem 277: 49605–49612.

Wang H, Brautigan DL. (2006). Peptide microarray analysis of substrate specificity of the transmembrane SER/THR kinase KPI-2 reveals reactivity with CFTR and phosphorylase. Mol Cell Proteomics 5: 2124–2130.

Waters KM, Le Marchand L, Kolonel LN, Monroe KR, Stram DO, Henderson BE et al. (2009). Generalizability of associations from prostate cancer genome-wide association studies in multiple populations. Cancer Epidemiol Biomarkers Prev 18: 1285–1289.

Wozniak MJ, Allan VJ. (2006). Cargo selection by specific kinesin light chain 1 isoforms. EMBO J 25: 5457–5468.

Zhou S, Zawel L, Lengauer C, Kinzler KW, Vogelstein B. (1998). Characterization of human FAST-1, a TGF beta and activin signal transducer. Mol Cell 2: 121–127.

Supplementary Information accompanies the paper on the Oncogene website (http://www.nature.com/onc)